CSMA 2022
15ème Colloque National en Calcul des Structures
16-20 Mai 2022, Presqu'île de Giens (Var)

Optimisation of blade shape for reducing vibration during tip-rub events

L. Salles[1,2], M. de Cherisey[2], A. Vizzaccaro[3,2]

[1] *Centre for Digital Engineering, Skoltech, Moscow, Russia, l.salles@skoltech.ru*
[2] *Imperial College London, UK,*
[3] *Bristol University, UK, alessandra.vizzaccaro@bristol.ac.uk*

Abstract —

Tip-rub events, also called blade-casing interactions, are problematic structural phenomena that can lead to complete engine failure. In this work the tip-rub phenomenon is studied through the prism of a promising physical quantity called clearance consumption, which allows to simply assess the behaviours of a blade experiencing blade-casing interactions. An automated workflows has been implemented in SALOME-MECA and its sub-modules, to perform simple and fast parametric studies and shape optimizations. The methodology is applied to a modified version of a NASA Rotor 37 blade and the influence of different geometry parameters is studied. The obtained results are compared to time domain simulation.

Mots clés — turbomachinery, vibration, tip-rub, optimisation, reduced order modelling

1 Introduction

While air traffic is expected to double in the next two decades, the International Air Transport Association (IATA), manufacturers and airlines have set a very challenging target to fight against climate change: cutting by 50% their global carbon emissions by 2050 (compared to 2005, [1]). To match this target and along with developing breakthrough solutions such as the hydrogen-powered aircraft, the aeronautical industry also focuses on improving every aspect of traditional airplanes. In particular, aircraft engines are required to be more and more efficient. In compressors especially, significant losses come from tip leakage flows. Because there is a clearance between the blade tip and the casing, a turbulent flow appears between the pressure and the suction side, creating important vorticity-induced losses. For compressors, a relevant improvement is therefore to close as much as possible the clearance between the blade tip and the casing to improve aerodynamics in the engine. It allows to reduce the losses mentioned above. However, minimizing this clearance is not costless as it turns an aerodynamics problem into a structural one. Because the engine casing is not perfectly circular (ovalization, asperities...) blade-casing interactions can occur.

For this reason, being able to predict blades response to tip-rub events and optimizing their shape regarding this problem is essential to the development of efficient and safe engines. Engine manufacturers have been trying to develop both numerical and experimental tools to accurately model and study this phenomenon. For example, Rolls-Royce in-house codes JM62 and FORSE, of which principles are respectively developed in [11] and [9] allow to assess different features related to blade-casing interactions: frequency and amplitude response, resulting forces and stresses, abradable material wear pattern as detailed in [11]. Although these solvers give precise and detailed results, they are very complex and computationally expensive to run, making them not really suitable for an early design and optimization stage. To this end, Batailly and Millecamps [2] suggested that a simple and unique quantity called the clearance consumption, which characterizes the evolution of the blade-casing clearance, could be used to assess the vibratory response of a blade following a tip-rub event. In this study we optimised the shape of the blade by minimising the clearance consumption and an tip rub event of the obtained optimised blade is simulated by time integration.

2 Methodology

2.1 Tiprub modelling

Tip-rub events can be studied using experimental test rigs or numerically modelled. As shown in [6], it is possible to experimentally measure different data related to tip-rub events: vibratory response (frequency and amplitude), stress/strain fields, wear patterns... But it is easier for manufacturers to run numerical simulations than physically test every configuration. Numerical models are also essential to perform parametric studies as the one later described in this work. Therefore, there have been many pieces of research conducted to correctly and efficiently model tip-rub events, using dynamic or static analysis.

2.1.1 Dynamic simulations

As the phenomenon of interest is a vibratory response following a shock (the tip-rub event(s)), blade-casing interactions are mainly studied using dynamic simulations. Rolls-Royce for example use two solvers: jm62 and FORSE which will be further discussed in this part. The problem can be mathematically formalized as the resolution of the equation of motion for the relevant system. For a time-dependent displacement field $\mathbf{U}(t)$:

$$\mathbf{M}\ddot{\mathbf{U}}(t) + \mathbf{C}\dot{\mathbf{U}}(t) + \mathbf{K}\mathbf{U}(t) = \mathbf{F_l}(t) + \mathbf{F_{nl}}(\dot{\mathbf{U}}(t), \mathbf{U}(t)) \tag{1}$$

where **M**, **C** and **K** are respectively the mass, damping and stiffness matrix of the system. For a contact problem, the forces are highly non-linear and can be decomposed into a linear (F_l) and a non-linear (F_{nl}) part.

2.1.2 Rubbing force estimation

The first step to solve 1 is to model the contact force. Different models have been developed depending on the desired computational efficiency and precision. They can be classified according to the three following categories: flexible blade and bare casing, flexible blade and coated casing (no wear taken into account), flexible blade and coated casing (wear taken into account).

In this study we used a flexible blade discretised by finite element and reduced using component mode synthesis. The Rubbing contact model relies on a penalty formulation of the contact. Apart from a new force expression, the particularity of this model is the use of a rotating frame (easier to compute as the blade degrees of freedom (DOF) do not have a rotational movement) but no wear model compared to Williams': only the deformation of the rigid casing is considered as a source of tip rubbing here.

Once the force is modelled and the model reduced, the general differential equation 1 has to be solved to complete the simulation. As always, depending on the desired output (FRF, vibratory modes, complete time response, stress fields...), the model can be reduced and the resolution simplified to enhance computational efficiency. For Rolls-Royce in-house codes, two solving processes can be used:

1. Time Integration Method in the in-house solver JM62 [11]
2. Harmonic Balance Method in the in-house solver FORSE [9]

Time integration methods are widely used to solve non-linear models including many DOFs. The solver jm62 used the implicit Newmark's method coupled with a newton solver for the contact non-linearities [11].

2.2 Mode shape and clearance consumption

2.2.1 Modal analysis

As previously pointed out, dynamic simulations are precise but complex and computationally expensive. Few recent studies [2, 4] use static modal analysis - which is much cheaper from a computational point of view - to study blade-casing interactions. This process allows to compute the natural frequencies at which a resonance might occur, and the associated modeshape of a system which shows how the system will deform. By performing a simple linear or non-linear modal analysis, it is possible to derive a quantity

called the clearance consumption which seems very promising regarding the assessment of the vibrations and possible resonances resulting from tip-rub events.

Linear resolution For the sake of brevity and clarity, one will consider equation 1 without the damping term (which is normally taken into account). The forcing term is also removed as one wants the natural frequencies of the system itself. However, the rotational load can be taken into account in a revised stiffness matrix if the system of interest is rotating:

$$\mathbf{M\ddot{U}} + \mathbf{KU} = \mathbf{0} \tag{2}$$

Assuming a periodic solution in the form $\mathbf{U} = \mathbf{u}e^{i\omega t}$, Eq. 2 can be simplified and re-written as an eigenvalues problem:

$$\left(\mathbf{M^{-1}K} - \omega^2\mathbf{I}\right)\mathbf{u} = \mathbf{0} \tag{3}$$

If the system has N degrees of freedom, solving this problem allows to access to N natural frequencies $f_i = \frac{\omega_i}{2\pi}$ (where ω_i are the N eigenvalues/natural pulsations) and eigenvectors/modeshapes ϕ_i. The latter can be used to study the trajectory of a point of a blade vibrating along mode i only: by projecting the vector ϕ_i associated to the DOF of the studied point on the radial and tangential directions (see Appendix 1 for the definition of the frames of reference and coordinate systems), the modal displacements can be computed. In the blade frame of reference, for mode i only:

$$\begin{cases} u_{i,r} = A(t)\phi_{i,r} \\ u_{i,\theta} = A(t)\phi_{i,\theta} \end{cases} \tag{4}$$

where r and θ indicate the radial and tangential components, respectively. A(t) is the time dependant amplitude. It has to be noticed that the variation of the radial displacement along the tangential one is linear as shown in Figure 1a below.

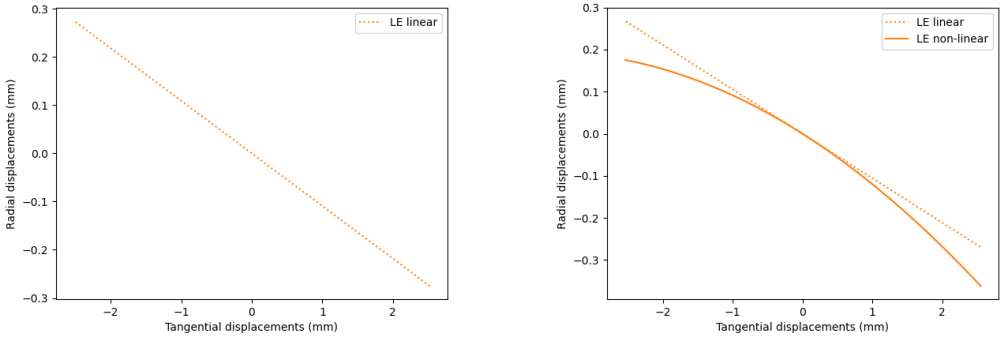

(a) Linear trajectory

(b) Non-linear trajectory

Figure 1: Linear trajectory of the leading edge of a custom compressor blade for the first bending mode for $A = 4 \cdot 10^{-4} \cos t$ where $t \in [0, \pi]$ and Non-linear trajectory of the leading edge of a custom compressor blade for the first bending mode for $A = 4 \cdot 10^{-4} \cos t$ where $t \in [0, \pi]$

Non-linear resolution: direct normal form As pointed out in the previous part, the basic modal analysis is derived from a linear differential equation and can therefore only predict linear trajectories. Using the direct normal form (DNF), it is possible to take into account geometric non-linearities when computing the modal displacements. To do so, quadratic and cubic non-linear terms g and h are added to Eq. 2:

$$\mathbf{M\ddot{U}} + \mathbf{KU} + g(\mathbf{U},\mathbf{U}) + h(\mathbf{U},\mathbf{U},\mathbf{U}) = 0 \tag{5}$$

The direct computations of the different modal coefficients is detailed in [5, 10]. this method allows to access to quadratic terms called second-order tensors a and b in addition to the linear modeshapes ϕ

detailed in the previous part. In the current project, we are interested in their projections on e_r and e_θ such as the radial and tangential displacements in the blade frame of reference due to the single mode i are equal to:

$$\begin{cases} u_{i,r} = A(t)\phi_{i,r} + A(t)^2 a_{i,r} + \dot{A}(t)^2 b_{i,r} \\ u_{i,\theta} = A(t)\phi_{i,\theta} + A(t)^2 a_{i,\theta} + \dot{A}(t)^2 b_{i,\theta} \end{cases} \tag{6}$$

As shown in Figure 1b, by taking into account non-linear terms, the model is able to produce more complex trajectories compared to the linear model.

In this non-linear analysis, centrifugal loading can also be taken into account as discussed in [5]. Compared to the linear modal analysis, it implicates more than just modifying the stiffness matrix: the computation of the different coefficients is also more complex.

2.2.2 Clearance consumption

Using the clearance consumption (c_c) as a way of studying tip-rub events was first introduced by Batailly and Millecamps in [2]. It is defined as the evolution of the distance blade tip/casing (or abradable coating if there is) when the blade is vibrating compared to the resting position. This distance is usually studied at specific tip positions such as leading edge, middle chord and trailing edge. Mathematically, the clearance consumption can be expressed as follows:

$$c_c = R(u_\theta) - R_0 \tag{7}$$

where $R(u_\theta)$ is the radial position of the studied point for a given tangential displacement u_θ and R_0 is the radial position at rest in the blade cylindrical frame of reference. Graphically, the quantity can be better understood with Figure 2a below. From the mathematical expression and the graphical explanation, it is clear that the clearance consumption exactly equals the radial displacement u_r introduced previously.

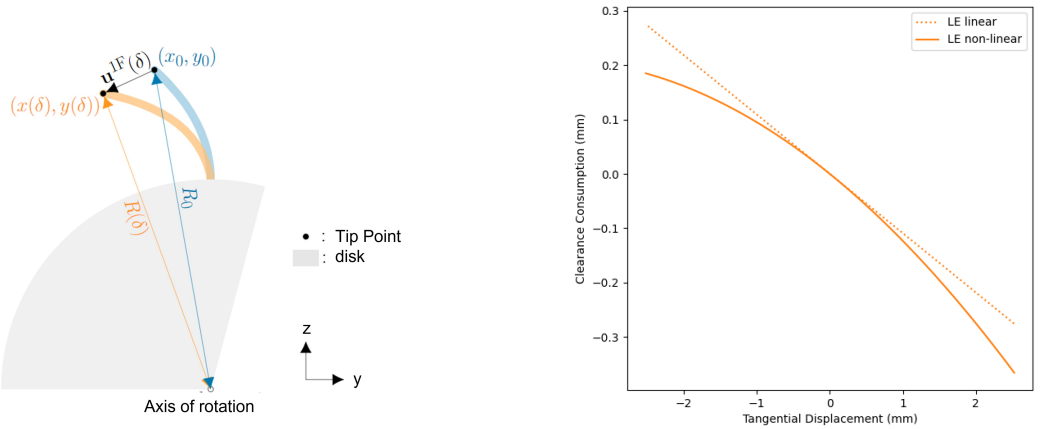

(a) Clearance consumption definition

(b) Clearance consumption of the leading edge

Figure 2: Clearance consumption definition (δ is the amplitude A introduced in Eq. 4) [4] and Clearance consumption of the leading edge of a custom compressor blade for the first bending mode for $u_t \in [-2.5, 2.5]$ mm

In [2], Batailly and Millecamps plotted the clearance consumption along the tangential displacement for each mode. The lower the clearance consumption, the better. In fact, if it is null or negative, it means that when the blade vibrates, the gap between the blade and the casing is increasing, making the tip less likely to rub on it. On the opposite, in Figure 2b, for negative tangential displacements, the clearance consumption is positive, which means that the gap between the blade tip and the casing is closing, making tip-rubbing more likely to happen. For a positive tangential displacement, the clearance consumption is negative and tip-rubbing is less likely to happen.

3 Testcase NASA Rotor 37 and General procedure

The compressor blade geometry from NASA Rotor 37 (NR37, detailed in [8, 3]) was selected as it is widely documented and used in this kind of preliminary studies [7]. The blade is represented in Figures 3a. It is made of 11 profiles stacked on a vertical and straight stacking line. In order to be able to easily control the shape of the blade, a simpler one (called Modified Nasa Rotor 37 (MNR37) in the following) was created from NASA Rotor 37, stacking only the mid-profile but on the same simple and straight stacking line). As visible in Figure 3b, the newly designed blade indeed presents the same stacking law compared to the reference. Following the experiments performed in [8], it was decided to use $\rho = 8000\ kg.m^{-3}$, $E = 180\ GPa$ and $\nu = 0.3$ where ρ, E, and ν are the density, Young's Modulus and Poisson's ratio, respectively.

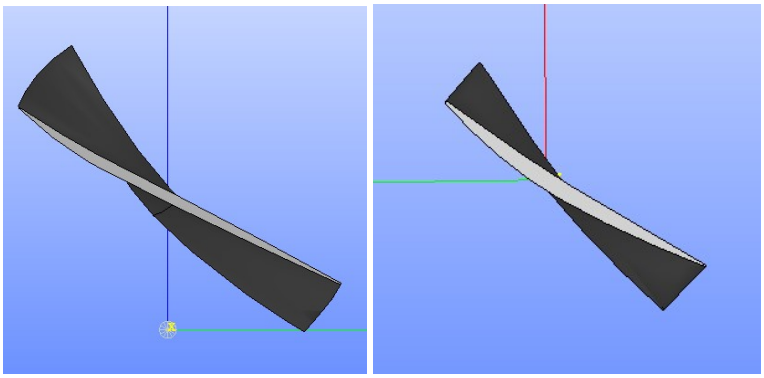

(a) Tip view of NASA Rotor 37 (b) Tip view of the MNR37

Figure 3: Compressor blade models

3.1 General procedure

The modal analysis used to compute the clearance consumption is done by processing the model, the mesh in SALOME submodules and the finite element solution in Code-Aster. Code-Aster has an interface in Python which makes easier the implementation of the operation required by the DNF and its integration in the different workflows. The DNF procedure is well explained in [10]. It allows to access both the linear and non-linear modal displacements as it exports the linear modeshapes and the second-order tensors introduced in 2.2.1. No gravity or aerodynamic loads are taken into account in this model.

3.1.1 Computing c_c and $c_{c,max}$

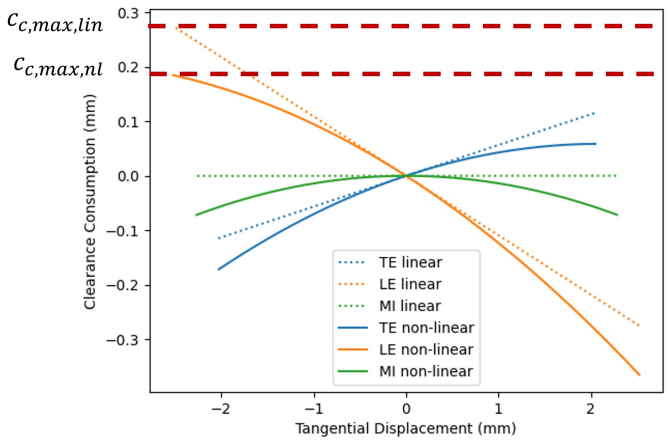

Figure 4: Clearance consumption for MNR37 for the first bending mode

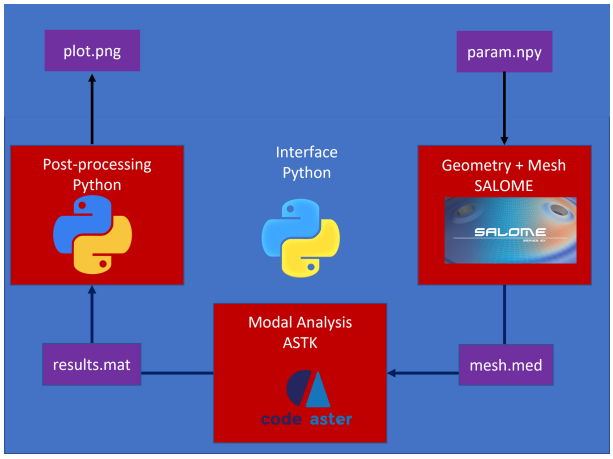

Figure 5: Objective function automated workflow

Once the modal analysis had been performed and the results had been exported, they could be post-processed to plot the clearance consumption for the tip leading edge (LE), trailing edge (TE) and middle chord (MI). As underlined in 2.2.2, the clearance consumption equals the radial displacements. Hence, it can be directly computed using eq. 4 (linear) and 6 (non-linear). In this study, the maximum acceptable tangential displacement was set to 2.5 mm, which corresponds to $\frac{1}{30}^{th}$ of the blade span length. This value was chosen to keep realistic displacements but big enough to see a difference between the linear and non-linear results.

From this limit, the amplitude can be derived for each mode. It is expressed as a sinusoid: $A(t) = A\cos t$ where $t \in [0,\pi]$. The scalar A is chosen such as the maximum tangential displacement for the leading edge, trailing edge or middle chord is equal to 2.5 mm. Mathematically:

$$A = \min_{p\in\{\text{LE,MI,TE}\}} A_p \text{ with } A_p \text{ such as } u_{\theta,p,max} = 2.5mm \tag{8}$$

Then the tangential displacements and the radial displacements c_c can be computed and plotted for each node (LE, TE, MI) using the amplitude derived previously. This kind of plot is shown in Figure 4. The maximum clearance consumption $c_{c,max}$ can be defined for the linear and non-linear case. It is represented in red dotted line in Figure 4. It is the maximum clearance consumption reached by any of the three nodes.

$$c_{c,max} = \max_{\substack{p\in\{\text{LE,MI,TE}\}\\ t\in[0,\pi]}} c_{c,p}(t) \tag{9}$$

In this study, only the three first modes were investigated as from the previous works on tip-rubbing cited before, they were supposed to be the most responding modes. Focusing on three modes only also allowed a fast computation of all the required data to compute c_c and $c_{c,max}$ for the different modes.

3.1.2 Optimization parameters

Because the objective function called the second meshing script, the optimization parameters were the twist, lean and sweep variation. The initial guess for the optimization process was chosen such as each parameter was set to the value giving the minimum $c_{c,max}$ in the parametric study.

The algorithmic architecture of the objective function was an automated version of the procedure for the parametric study. The workflow is presented in Figure 5. The objective function takes as an argument a triplet containing the desired fraction of variation for the twist, lean and sweep and returns the maximum clearance consumption for the first bending mode.

3.2 Time domain simulation

The dynamic simulation aimed at producing an interaction map. To do so, one needed to introduce a source of tip-rubbing and do a rotational speed sweep. The numerical time integration simulates a five seconds period of time with a time step of $5 \cdot 10^{-5} s$ and proceeds as shown in Figure 6

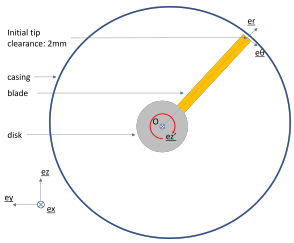

(a) Scenario for $0 \leq t < 2$ and $4 < t \leq 5$

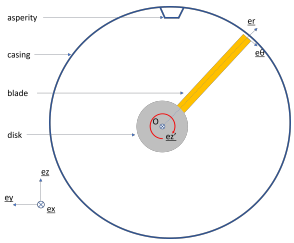

(b) Scenario for $2 \leq t \leq 4$

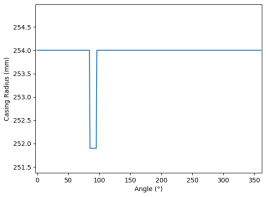

(c) Casing profile for $2 \leq t \leq 4$

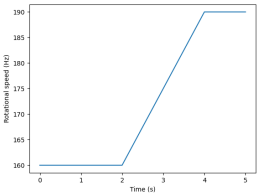

(d) Rotational speed profile

Figure 6: time domain simulation scenario

4 Results for an optimised blade

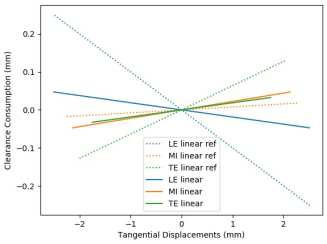

(a) Mode 1B

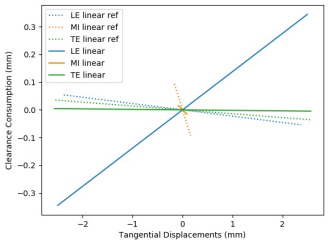

(b) Mode 1T

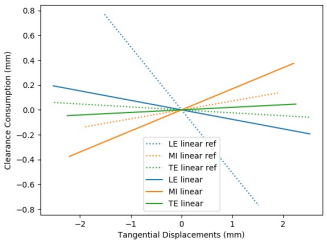

(c) Mode 2B

Figure 7: Clearance consumption of the optimized blade 2

From the initial guess of [-0.3, -0.03, 0.3] the Python procedure returned the triplets [-0.3, -0.0222, -0.3] i.e. compared to MNR37, a blade untwisted by 30%, with a 2.22% chord length negative lean and a 30% chord length forward sweep. The associated clearance consumption for the first three modes is plotted in Figure 7.

4.1 Tiprub event for the optimised blade

Finally, the optimised blade is tested using the time donain solver jm62 to confirm that, as for the clearance consumption, higher optimization bounds means greater effects. The associated interaction maps are plotted in Figure 8. For the multi-contact case, the mode 1B interaction zone has nearly disappeared as the maximum amplitude is divided by 6 compared to MNR37 but a small zone that was nonexistent can also be noticed for mode 1T.

5 Conclusions

The study has shown that the clearance consumption is a promising and relevant quantity to characterise the response of compressor blade to tip-rub events and to build automated workflows to study and optimize these blades. The promising processes developed in this work can be improved by building a more complex parametric model based on multi-objective optimisation to generate blade geometries and by considering geometric non-linear effects both in the modal analysis and dynamic simulations.

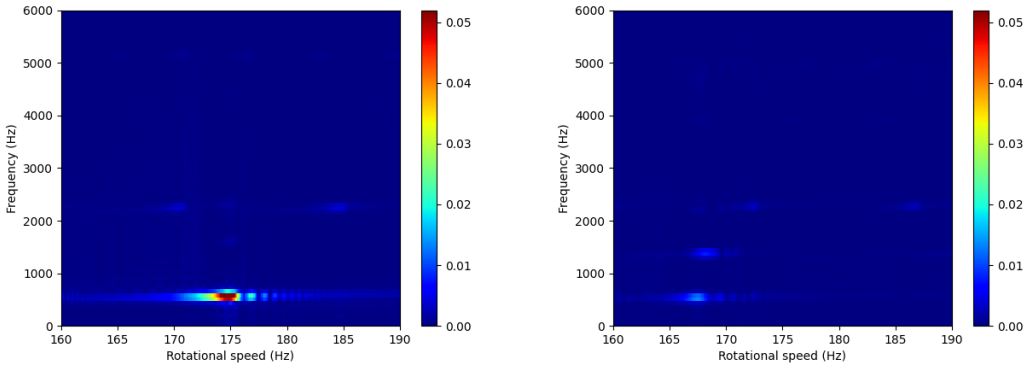

(a) MNR37 (b) Optimized blade 2

Figure 8: Interaction maps of the tip leading edge radial displacements for contact case

References

[1] *Aircraft Technology Roadmap to 2050*. Tech. rep. International Air Transport Association, 2009.

[2] Alain Batailly and Antoine Millecamps. "Minimising clearance consumption: a key factor for the design of blades robust to rotor/stator interactions?" In: *ASME Turbo Expo*. Séoul, South Korea, June 2016. DOI: 10.1115/GT2016-56721.

[3] J. Crouse. "Computer program for definition of transonic axial-flow compressor blade rows". In: (1974).

[4] Julien Lainé. "Optimisation d'aubes de turbomachines : minimisation de la réponse vibratoire à la suite de contacts avec le carter". MA thesis. Dec. 2017, p. 94. URL: https://dumas.ccsd.cnrs.fr/dumas-01737838.

[5] A. Martin et al. "Réduction de modèle en dynamique non linéaire par la méthode de paramétrisation des variétés invariantes – Application au cas des structures tournantess". In: Giens, France, May 2022.

[6] Antoine Millecamps et al. "Snecma's Viewpoint on the Numerical and Experimental Simulation of Blade-Tip/Casing Unilateral Contacts". In: *ASME Turbo Expo Conference*. Proceedings of the ASME Turbo Expo 2015. ASME. Montréal, Canada, June 2015. DOI: 10.1115/GT2015-42682.

[7] Elsa Piollet, Florence Nyssen, and Alain Batailly. "Blade/casing rubbing interactions in aircraft engines: Numerical benchmark and design guidelines based on NASA rotor 37". In: *Journal of Sound and Vibration* 460 (2019), p. 114878. ISSN: 0022-460X. DOI: https://doi.org/10.1016/j.jsv.2019.114878.

[8] L. Reid and R. Moore. "Design and overall performance of four highly loaded, high speed inlet stages for an advanced high-pressure-ratio core compressor". In: (1978).

[9] Loic Salles. *Development of a new rubbing element in jm62/FORSE*. Tech. rep. 2015.

[10] Alessandra Vizzaccaro et al. "Direct computation of nonlinear mapping via normal form for reduced-order models of finite element nonlinear structures". In: *CoRR* abs/2009.12145 (2020). arXiv: 2009.12145. URL: https://arxiv.org/abs/2009.12145.

[11] Robin Williams. "Simulation of Blade Casing Interaction Phenomena in Gas Turbines Resulting From Heavy Tip Rubs Using an Implicit Time Marching Method". In: *ASME 2011 Turbo Expo: Turbine Technical Conference and Exposition*. Vancouver, Canada, June 2011. DOI: 10.1115/GT2011-45495.